Optical determination of the effective wetting layer thickness and composition in InAs/Ga(In)As quantum dots

M. Hugues,[1] M. Teisseire,[1] J.-M. Chauveau,[1,2] B. Vinter,[1,2] B. Damilano,[1] J.-Y. Duboz,[1] and J. Massies[1]
[1]*Centre National de la Recherche Scientifique, Centre de Recherche sur l'Hétéro-Epitaxie et ses Applications, rue B. Grégory, 06560 Sophia Antipolis, France*
[2]*Physics Department, University of Nice-Sophia Antipolis, 06108 Nice Cedex 2, France*
(Received 20 April 2007; revised manuscript received 14 June 2007; published 21 August 2007)

A different approach to determining the wetting layer thickness and composition in InAs/Ga(In)As quantum dot systems is proposed. This method combines the energy separation between heavy and light hole states determined experimentally and the results of a simple envelope function calculation to unambiguously obtain the wetting layer parameters. The heavy and light hole states are probed by photoluminescence excitation, but the proposed method can be extended to all absorptionlike measurements. For InAs/GaAs quantum dots, an *effective* wetting layer thickness of 3.6 monolayers and an average indium composition of 43% are obtained, in good agreement with results of structural characterization. Moreover, the optical transitions for InAs quantum dots covered by a 5 nm thick (Ga,In)As cap layer with indium content up to 20% have also been probed. Several transitions resulting from the quantum well formed by the wetting layer and the cap layer have been detected. Using the wetting layer parameters deduced for InAs/GaAs quantum dots, the calculated e_1-hh_1, e_1-lh_1, e_1-hh_2, and e_2-hh_2 transition energies correspond very well with the peak energies of the photoluminescence excitation spectra.

DOI: 10.1103/PhysRevB.76.075335 PACS number(s): 73.21.La, 78.67.−n, 78.55.−m

I. INTRODUCTION

During the past decade, self-assembled semiconductor quantum dots (QDs) have attracted considerable interest due to their fundamental physics and various potential applications such as laser diodes and detectors.[1,2] The three-dimensional carrier confinement and the deltalike density of states of these nanostructures result in lower laser threshold current density but also open the way to novel applications such as single electron transistors and single photon sources.[3,4] The starting point of this already long story is that in some highly lattice-mismatched heterostructures such as InAs on GaAs, the occurrence of the Stranski-Krastanow (SK) growth mode leads to the formation of dislocation-free self-assembled islands. The driving force for this self-assembling mechanism is the balance between the strain energy inside the deposited layer and the surface energies of the substrate, the layer, and the interface. The growth mechanism of these islands has been widely studied experimentally[5,6] and theoretically,[7,8] resulting in several different theories. However, the growth mechanism can be simply described as follows. During SK growth, first a thin two-dimensional layer is formed with a strain energy increasing with its thickness. Above a critical thickness, which is around 1.5–1.7 monolayer (ML) for InAs on GaAs, island formation begins, resulting in partial elastic strain relaxation at the island free surface, which overcompensates the energy cost induced by the increase of the surface energy. This growth mode finally results in three-dimensional QDs on top of a two-dimensional wetting layer. The optical and electrical properties of this system are mainly determined by the electronic states of the dots, but can be greatly affected by the wetting layer (WL). For instance, the WL can behave as a channel for carrier redistribution between the dots, allowing the achievement of a common quasiequilibrium Fermi distribution in a QD ensemble.[9] Moreover, several temperature-dependent optical studies have shown that the decrease of the photoluminescence (PL) intensity with increasing temperature is induced by electron-hole pair escape from the QDs to the WL.[10,11] The WL can affect the dark current in QD detectors[12] and it was also predicted that it could limit the modulation response of QD lasers.[13] However, despite the significant role of the WL on the QD optical properties, the determination of the WL parameters (i.e., indium composition and thickness) remains very difficult. Indeed, the WL parameters are generally obtained by high-resolution transmission electron microscopy (HRTEM) or cross-sectional scanning tunneling microscopy (X-STM).[14,15] Recently, the observation of heavy and light hole related transitions in photoreflectance spectra has been used to determine the WL thickness by comparing the experimental data with the results of envelope function calculations.[16] However, they have used the nominal In content for their calculations despite the composition change commonly observed during the QD formation and subsequent cap layer growth.[14,15,17] In this paper, we show that it is possible to deduce unambiguously the effective WL thickness and composition (i.e., after QD encapsulation) by the combination of photoluminescence excitation (PLE) measurements and transition energy calculations using the envelope function method. The principle of our method can also be applied by using photoreflectance instead of PLE. The WL parameters obtained with our approach are in good agreement with the results obtained from transmission electron microscopy (TEM) measurements. Finally, InAs QDs covered by 5 nm thick (Ga,In)As cap layers with indium contents ranging from 0 to 20% have also been studied. The experimental transition energies of the quantum wells (QWs) formed by the WL and the cap layers are in accordance with those calculated with the WL parameters obtained for InAs/GaAs QDs.

II. EXPERIMENT

The samples studied in this work were grown by molecular beam epitaxy in a Riber 32P reactor on 2 in. GaAs substrate using solid sources. After the deoxidation of the substrate at 600 °C, a 700 nm thick GaAs buffer layer was grown at 580 °C. After 10 min annealing at 580 °C in order to smooth the surface, the growth temperature was cooled down to 520 °C for the deposition of 2.4 ML of InAs. Then, the growth was interrupted and the substrate temperature was decreased to 420 °C for the growth of a 5 nm thick Ga(In)As cap layer and a subsequent 5 nm thick GaAs layer. The In content in the cap layer was varied from 0 to 20%. After the growth of the cap layer, the substrate temperature was increased to 580 °C for the deposition of 100 nm thick GaAs.

Room temperature PL measurements were carried out using the 514.5 nm line of an Ar^+ laser, while a tunable Ti:sapphire laser was used for PLE characterizations at 2 K, both in the near backscattering geometry. The PL and PLE spectra were measured using a liquid nitrogen cooled Ge detector located at the exit of a 64 cm single and 1 m double monochromators, respectively. The TEM cross-section sample was conventionally prepared with Ar^+ ion milling but using a low energy of 100 V in the final stage, in order to minimize amorphous layer generation which limits the accuracy of the local composition evaluation.[14] A JEOL 2010 field-emission gun microscope operating at 200 kV was used for cross-section dark-field images using {002} reflection and {110} zone axis for HRTEM images.

III. RESULTS AND DISCUSSION

A. Optical determination of InAs/GaAs effective wetting layer parameters

The wetting layer thickness and composition are generally deduced from structural characterizations which require much experimental and simulation work. We propose to use a different, convenient, and fast optical determination of the InAs/GaAs WL parameters. For InAs/GaAs QDs, a high energy peak (around 1.33 eV at room temperature and 1.42 eV at 10 K) appears in the PL spectra and was attributed to carrier recombinations in the WL (i.e., e_1-hh_1 transition).[18,19] However, using band diagram calculations, the same transition energy can be obtained with different sets of In content–WL thickness. In order to remove this ambiguity, we use PLE and transition energy calculations. The idea is to use the energy difference between the transitions involving light (lh) and heavy holes (hh) (i.e., e_1-lh_1 and e_1-hh_1). Indeed, in addition to the difference between the heavy and light hole effective masses, the shear strain component resulting from the lattice mismatch between GaAs and the WL leads to an increase of the splitting between the heavy and light hole valence bands.[20] So, this energy separation will correspond to only one WL configuration. Figure 1 shows the room temperature PL spectra with an excitation power density of 30 W/cm^2. The QD ground-state transition is centered at 0.991 eV with a full width at half maximum of 30 meV, while additional peaks are present at 1.068 and

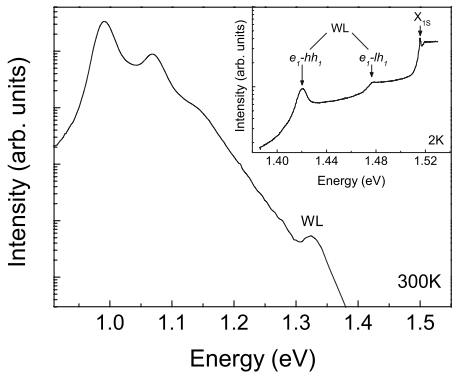

FIG. 1. Room temperature PL spectrum of InAs/GaAs quantum dots. The inset shows the 2 K PLE spectrum of the same sample with the detection energy at the maximum of the QD ground-state PL intensity.

1.132 eV. The latter two peaks progressively disappear as the excitation power density decreases, so they are induced by state filling and correspond to QD excited states.[21] Another peak appears also at much higher energy (1.325 eV), corresponding to carrier recombinations in the WL. Note that the PL intensity of the WL peak is nearly 4 orders of magnitude lower than the QD ground-state intensity, indicating that the carriers present in the WL are efficiently transferred into the QDs. Moreover, independent of the excitation power density, no PL signal from the WL has been detected at low temperature. The inset in Fig. 1 shows the 2 K PLE spectrum of the same sample with the detection energy at the maximum of the QD ground-state PL intensity. In addition to the 1*s* state of the bulk GaAs exciton peak at 1.515 eV (X_{1S}), the peaks at 1.4204 and 1.4778 eV are typical for excitonic transitions in a QW and can be attributed to the heavy (e_1-hh_1) and light (e_1-lh_1) hole transitions in the WL.[19,22,23] The heavy and light hole characters of these transitions have been revealed in the past by polarization-dependent PL and PLE spectroscopy in the edge-emission and edge-excitation modes.[24] Band diagram calculations have been carried out in order to determine the different sets of In content and WL thickness which give the same e_1-hh_1 transition energy as the PLE measurement (1.4204 eV at 2 K). For this calculation, only the first electron and heavy hole state energies are required, so a "simple" one-band $k \cdot p$ model using the envelope function approximation is sufficient. The exciton binding energy was taken into account and was computed by using an analytical equation deduced from variational wave function calculations.[25] The values of the band gaps, effective masses, deformation potentials, and elastic constants have been deduced from linear interpolation between the GaAs and InAs values.[26] A square QW, without In segregation, has been considered at first approximation. The curve reported in Fig. 2(a) represents the different sets of composition and thickness giving the same e_1-hh_1 transition energy as the one measured by PLE. Then the energy separation between the heavy and light hole states of the WL must be calculated for the different configurations (composition-thickness) reported in Fig. 2(a). For the calculation of the light hole state position, a more complicated 18-band $k \cdot p$ model was used in order to take into account the coupling

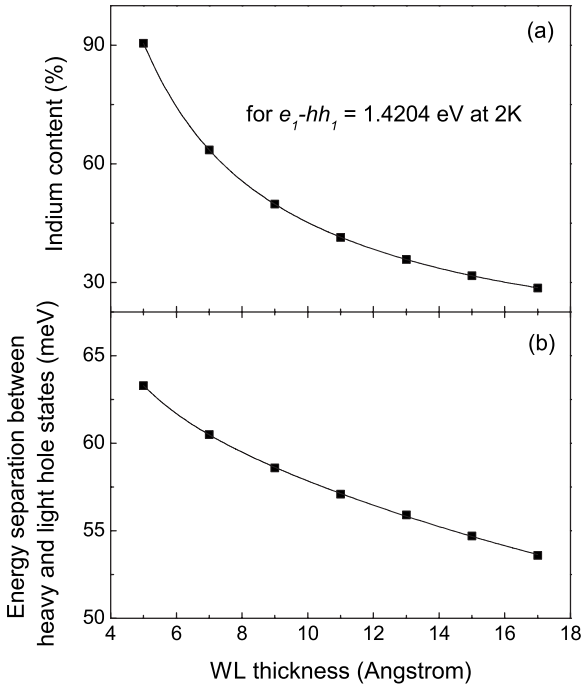

FIG. 2. (a) Indium content and (b) energy separation between heavy and light hole states as a function of the WL thickness calculated for a fixed e_1-hh_1 transition energy of 1.4204 eV at 2 K. Each point in (b) corresponds to a couple of WL thickness–In content. For a given WL thickness, the In content associated is reported in (a).

between valence bands and the spin-orbit splitting. Details about the 18-band $k\cdot p$ formalism used in this study can be found in Ref. 27. These calculations show that the high compressive strain pushes the light hole state very close to the GaAs band edge for all the WL configurations, in good agreement with the results reported for single-monolayer InAs/GaAs QWs and (Ga,In)As/GaAs superlattices.[24,28] Moreover, the fact that the WL light holes are in the vicinity of the GaAs band edge can explain the observed broadening of the e_1-lh_1 transition in the PLE spectrum (inset in Fig. 1). This result is very interesting since the light hole position can be approximated to be the GaAs valence band edge. In this case, the energy separation between the first light and heavy hole states corresponds to $\Delta E_V - \mathrm{hh}_1$ (ΔE_V is the valence band offset between the WL and the GaAs) and can be directly obtained from the one-band $k\cdot p$ calculations used to determine the different composition-thickness sets reported in Fig. 2(a). Figure 2(b) shows the energy separation between the heavy and light hole states thus obtained for the different WL configurations determined previously. While all the WL configurations give the same e_1-hh_1 transition energy, the hh-lh energy separation is not constant, which allows us to determine the WL thickness and composition unambiguously. From Fig. 2(b), the 57.4 meV energy separation deduced from the PLE measurement corresponds to a WL thickness of 10.6 Å (≅3.6 ML). By using this thickness, an In composition of around 43% can be determined from Fig. 2(a). Despite some differences in the growth conditions, the In content thus obtained is in the same range as those

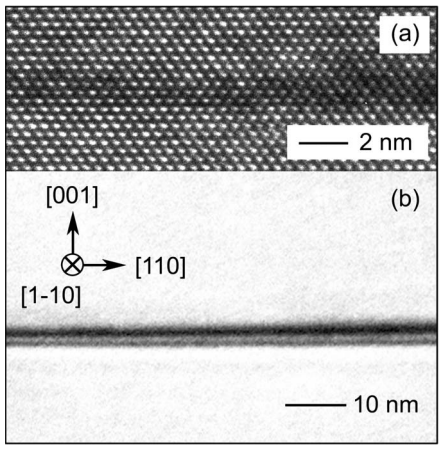

FIG. 3. (110) cross-section (a) HRTEM image and (b) dark-field image taken under conditions with a diffraction vector $\mathbf{g}=(002)$.

already reported for TEM and X-STM measurements [between 25% and 35% (Refs. 14 and 15)] and is in excellent agreement with the value deduced from x-ray diffraction measurements of QD stacks grown by metal organic chemical vapor deposition.[29] Moreover, if these values are converted to an equivalent pure InAs layer, the thickness thus obtained is 1.6 ML, in good agreement with the critical thickness generally reported in the InAs/GaAs system.[6,30] An assumption able to explain this result would be that the mass transfer between the WL and the QD is negligible.[31] However, another explanation can be that the In atoms transferred from the indium layer at the WL surface to the QDs are partially compensated by the In atoms coming from the dissolution of the QD top during the capping process.[15,17] However, the larger thickness and lower In content compared to a pure InAs WL indicate that In segregation[14,15] or intermixing during the cap layer growth occurs, such as for Ge/Si islands.[32] These processes should modify the confinement potential significantly, possibly discrediting the square well approximation used in the calculations. So, a structural characterization is necessary in order to assess the validity of the square well approximation and also the validity of our method.

B. Structural determination of InAs/GaAs wetting layer parameters

To obtain the indium profile of the WL, TEM measurements have been carried out. Figure 3(a) displays a high-resolution image taken from the WL in a ⟨110⟩ zone axis. The growth direction (i.e., the [001] direction) is indicated in the figure. The dark contrast is due to a high In concentration, locating therefore the WL position. The WL is asymmetrical with a straight bottom interface and a diffuse upper interface. Under these TEM conditions, it is possible to estimate the WL width to be between 3 and 4 ML, in very good agreement with the 3.6 ML deduced in Sec. III A. The local In profile through the WL was deduced from dark-field images using the chemical composition sensitive {002} reflection [Fig. 3(b)]. In these experimental conditions, the contrast is directly related to the In composition profile.[33] In

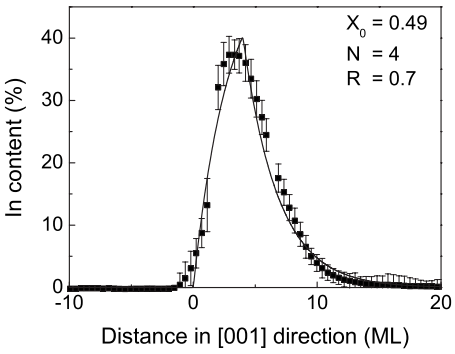

FIG. 4. Indium concentration profile in the growth direction obtained by averaging in 40 nm wide regions of the WL. The squares are the experimental data from TEM investigation and the solid curve is calculated by using the segregation model of Muraki *et al.*

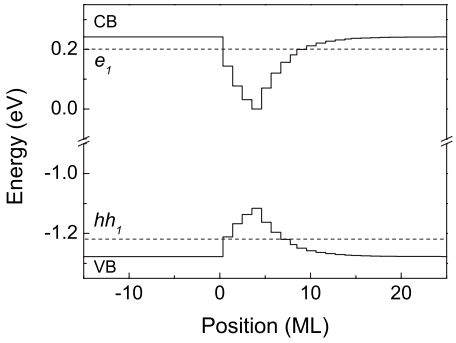

FIG. 5. Calculated band diagram with the segregated In profile. Only the first quantized levels of electrons e_1 and holes hh_1 are represented.

order to reduce the noise due to the surface amorphous layer, particular attention has been paid to the final stage of the sample preparation by using a very low voltage for the ion milling (100 V). The intensity profile along the [001] direction was averaged over 40 nm along the [110] direction in order to further reduce the noise. The experimental error was estimated as the maximum deviation of the intensity to the average value. The In profile was deduced from the intensity profile following the procedure described in Ref. 34. Finally, the distance was calibrated in ML units, taking into account the In composition and the pseudomorphic strain relaxation along the [001] direction. Figure 4 shows the indium concentration profile thus obtained (squares), where the zero point of the abscissa corresponds to the interface between the GaAs buffer layer and the WL. The profile is clearly not symmetrical, presenting a slower decay toward the GaAs cap layer. This allows us to rule out any interdiffusion mechanism and seems to indicate the occurrence of In surface segregation.[35–38] So, we have described the indium composition with the phenomenological model of Muraki *et al.*,[36] which assumes that during growth a certain fraction R of In atoms on the topmost layer segregates to the next layer, while only $(1-R)$ is incorporated into the bulk before the next ML is completed. The solid line in Fig. 4 is the In profile obtained with a nominal In content $x_0=49\%$, a nominal WL thickness $N=4$ ML, and a segregation coefficient $R=0.7$. These nominal In content and WL thickness values are in good agreement with the ones obtained in Sec. III A. However, the segregation coefficient R is lower than the typical 0.8–0.85 values reported for In segregation in WL.[14,15] Our low segregation coefficient value is mainly due to the low cap layer growth temperature (i.e., 420 °C for the first 10 nm of the cap layer) since many studies on (Ga,In)As and (Ga,In)P QWs have demonstrated that the In segregation decreases as the growth temperature decreases.[35–37] Therefore, in addition to the blueshift reduction of the QD emission energy induced by the low cap layer growth temperature,[38] the wetting layer thickness broadening is also minimized. A larger energy separation between the QD and WL states (i.e., higher barrier height) can be expected, thus reducing the QD carrier escape process.[10] A band diagram calculation has been carried out using the WL In profile deduced from the TEM investigation (Fig. 5). The In profile was discretized into monolayer step and the confined energy levels were obtained by solving the Schrödinger equation with the transfer matrix method. The calculated e_1-hh_1 transition energy taking into account the exciton binding energy is 1.406 eV, corresponding to a difference of 14 meV with the experimental value. The energy separation between heavy and light hole states is 58.3 against 57.4 meV from PLE measurement. This difference roughly represents an error of 4% on the composition and only 1 Å on the WL thickness (Fig. 2). This result corroborates the theoretical study of Schowalter *et al.*, in which it was found that the optical properties are only significantly affected by segregation for R and N higher than 0.7 and 5 ML, respectively.[39] As a consequence, the error induced by the square well approximation can be neglected, thereby allowing the extraction of the WL parameters directly from the PLE measurement.

C. InAs/(Ga,In)As structures

Many optical and structural studies of the effects of the growth conditions on the effective WL parameters have been reported. Among these, X-STM measurements have shown that the In segregation coefficient R, in other words the WL thickness, is independent of the InAs growth rate or the amount of deposited InAs.[15] On the other hand, there is a controversy concerning the effect of the growth interruption duration applied before the cap layer deposition. A clear decrease of the maximum In content with increasing interruption time has been observed on composition profiles deduced from TEM measurements,[14] while PLE experiments have shown that the WL heavy and light hole transition energies both remain fixed, independent of the growth interruption time.[19] Despite all these experiments, the effect of a (Ga,In)As cap layer on WL parameters has never been elucidated because of the difficulty to discriminate the WL and the cap layer in structural measurements. Figure 6 shows the PLE spectra for InAs QDs covered by 5 nm thick $Ga_{1-x}In_xAs$ layers with x ranging from 0 to 20%. The gap in the spectra between 1.365 and 1.386 eV for the higher two In contents is due to the change of the mirrors used for the Ti:sapphire laser to reach this wavelength range. Note that

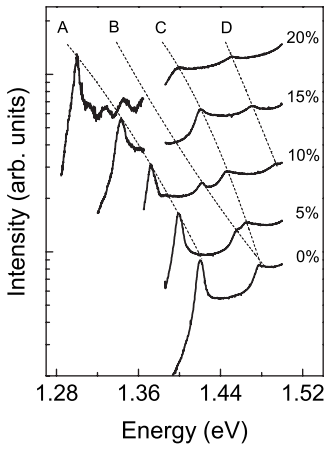

FIG. 6. 2 K PLE spectra for InAs QDs covered by 5 nm thick $Ga_{1-x}In_xAs$ cap layers with x ranging from 0 to 20%. The dashed lines are guides for the eyes and correspond to the four different peaks labeled *A*, *B*, *C*, and *D*.

the PLE spectrum for $x=10\%$ is continuous: in this case, the mirror change was very carefully carried out in order to resolve the low energy peak. The different peaks have been labeled from *A* to *D*. All the peaks redshift as the In content in the cap layer increases, implying that they are all related to the quantum well formed by the WL and the (Ga,In)As cap layer. From the study of the InAs/GaAs sample (Sec. III A), peaks *A* and *C* can already be assigned to e_1-hh_1 and e_1-lh_1 transitions, respectively. Peak *B* is clearly visible for $x=5\%$ and 10%, while it corresponds to a very weak bump, only visible when a zoom is carried out, for $x=0$ and 15%. The last peak *D* appears at higher energy when the In content is higher than 5%. Some other peaks at 1.328 and 1.346 eV appear for the sample with the highest In content. The origin of these peaks may be light absorption at the intermixed interface between the $Ga_{0.8}In_{0.2}As$ cap layer and the GaAs,[40] indium inhomogeneity in the cap layer, or phonon resonances.[23] Moreover, the QD ground-state PL intensity at room temperature is weaker for these sample,[11] probably because some defects acting as nonradiative recombination centers appear in the cap layer or in the GaAs barrier.[11,40] In order to assign the peaks from *A* to *D* to their corresponding transitions, band diagram calculations using the method of Sec. III A have been carried out. The WL parameters obtained for InAs/GaAs sample and the nominal (Ga,In)As cap layer thickness and In content have been used. The transition energies thus obtained are reported in Fig. 7 (dashed lines). As can be seen, peaks *A* (up triangles) and *C* (down triangles) correspond very well with the calculated transition energies e_1-hh_1 and e_1-lh_1, respectively. Peak *B* (circles) is in good agreement with a transition involving the first electron state and the second heavy hole state (i.e., e_1-hh_2). This transition is parity forbidden for a perfectly square QW, but becomes allowed in a $GaAs/Ga_{1-y}In_yAs/Ga_{1-x}In_xAs/GaAs$ asymmetrical QW (i.e., y and x being the In contents in the WL and the cap layer, respectively). For the sample capped with GaAs, this transition is very weak but allowed, owing to the asymmetry induced by the In segregation (Sec. III B). Note that the observation of this transition shows that the

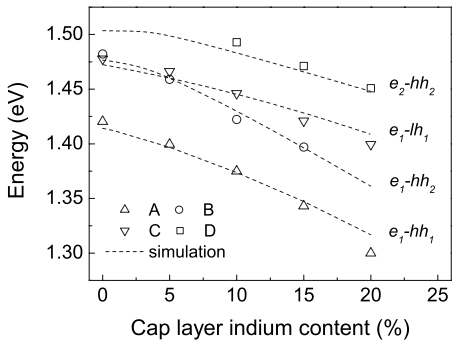

FIG. 7. Energies of *A* (up triangles), *B* (circles), *C* (down triangles), and *D* (squares) peaks as a function of the indium content in the cap layer. The dashed lines are the calculated e_1-hh_1, e_1-lh_1, e_1-hh_2, and e_2-hh_2 transition energies using the WL parameters determined for InAs/GaAs QDs ($x_{In}=43\%$ and thickness=3.6 ML) and the nominal cap layer parameters.

absorptionlike character of PLE allows probing optical transitions with very low oscillator strength. The last peak *D* (squares) appears for In content higher than 5% and corresponds to the transition between the second electron and heavy hole states (e_2-hh_2). The most interesting point is that good agreement between the calculations and all the transition energies obtained by PLE is obtained using the WL parameters deduced for QDs covered by a GaAs cap layer. This allows us to conclude that the introduction of In in the cap layer has a negligible effect on the effective WL thickness and composition [at least when the GaAs and (Ga,In)As cap layer growth conditions are the same]. Moreover, this agreement also confirms that when the cap layer growth temperature is sufficiently low to restrict the In segregation, the approximation of a square well can be used to model the WL with the parameters deduced from PLE measurements and band diagram calculations.

IV. CONCLUSION

A method combining band diagram calculations and photoluminescence excitation measurements has been proposed to determine the effective wetting layer thickness and composition. This approach uses the energy separation between heavy and light hole states to obtain the wetting layer parameters unambiguously. For InAs quantum dots covered by a GaAs cap layer, our method gives a wetting layer thickness of 3.6 ML and an average indium composition of 43% that is in good agreement with the structural characterization. We have shown that the square well approximation can be applied for our growth conditions, which correspond to the indium segregation coefficient of around 0.7, as deduced from the transmission electron microscopy investigation. Indeed, with this low coefficient, segregation has a negligible impact on the transition energies. On the other hand, photoluminescence excitation measurements on InAs quantum dots covered by (Ga,In)As cap layers with indium content up to 20% have been carried out. Using the wetting layer parameters obtained for GaAs cap layer, the absorption peak energies are in good agreement with the calculated e_1-hh_1,

e_1-lh_1, e_1-hh_2, and e_2-hh_2 transition energies. At least for the low cap layer growth temperature used in this work, a (Ga,In)As instead of GaAs cap layer does not change significantly the effective wetting layer thickness and composition. Finally, we can add that in addition to its relative simplicity, the proposed method can be extended to all absorptionlike measurements, allowing to probe the heavy and light hole states.

ACKNOWLEDGMENT

This work is partially supported by the French Ministry of Research (AC nanosciences BAND) project.

[1] I. R. Sellers, H. Y. Liu, T. J. Badcock, K. M. Groom, D. J. Mowbray, M. Gutiérrez, M. Hopkinson, and M. S. Skolnick, Physica E (Amsterdam) **26**, 382 (2005).
[2] J. Phillips, J. Appl. Phys. **91**, 4590 (2002).
[3] F. Hofmann, T. Heinzel, D. A. Wharam, J. P. Kotthaus, G. Böhm, W. Klein, G. Tränkle, and G. Weimann, Phys. Rev. B **51**, 13872 (1995).
[4] D. C. Unitt, A. J. Bennett, P. Atkinson, D. A. Ritchie, and A. J. Shields, Phys. Rev. B **72**, 033318 (2005).
[5] H. Kitabayashi and T. Waho, J. Cryst. Growth **150**, 152 (1995).
[6] J. M. Gérard, J. B. Génin, J. Lefebvre, J. M. Moison, N. Lebouché, and F. Barthe, J. Cryst. Growth **150**, 351 (1995).
[7] C. Priester and M. Lannoo, Phys. Rev. Lett. **75**, 93 (1995).
[8] N. Moll, M. Scheffler, and E. Pehlke, Phys. Rev. B **58**, 4566 (1998).
[9] S. Sanguinetti, T. Mano, M. Oshima, T. Tateno, M. Wakaki, and N. Koguchi, Appl. Phys. Lett. **81**, 3067 (2002).
[10] E. C. Le Ru, J. Fack, and R. Murray, Phys. Rev. B **67**, 245318 (1999).
[11] M. Hugues, M. Richter, B. Damilano, J.-M. Chauveau, J.-Y. Duboz, J. Massies, and A. D. Wieck, Phys. Status Solidi C **3**, 3979 (2006).
[12] J.-Y. Duboz, H. C. Liu, Z. R. Wasilewski, M. Byloss, and R. Dudek, J. Appl. Phys. **93**, 1320 (2003).
[13] D. G. Deppe and D. L. Huffaker, Appl. Phys. Lett. **77**, 3325 (2000).
[14] A. Rosenauer, W. Oberst, D. Litvinov, D. Gerthsen, A. Förster, and R. Schmidt, Phys. Rev. B **61**, 8276 (2000).
[15] P. Offermans, P. M. Koenraad, R. Nötzel, J. H. Wolter, and K. Pierz, Appl. Phys. Lett. **87**, 111903 (2005).
[16] P. Poloczek, G. Sek, J. Misiewicz, A. Löffler, J. P. Reithmaier, and A. Forchel, J. Appl. Phys. **100**, 013503 (2006).
[17] F. Ferdos, S. Wang, Y. Wei, A. Larsson, M. Sadeghi, and Q. Zhao, Appl. Phys. Lett. **81**, 1195 (2002).
[18] S. Sanguinetti, M. Henini, M. Grassi Alessi, M. Capizzi, P. Frigeri, and S. Franchi, Phys. Rev. B **60**, 8276 (1999).
[19] U. W. Pohl, K. Pötschke, A. Schliwa, F. Guffarth, D. Bimberg, N. D. Zakharov, P. Werner, M. B. Lifshits, V. A. Shchukin, and D. E. Jesson, Phys. Rev. B **72**, 245332 (2005).
[20] S. L. Chuang, Phys. Rev. B **43**, 9649 (1991).
[21] S. Fafard, R. Leon, D. Leonard, J. L. Merz, and P. M. Petroff, Phys. Rev. B **52**, 5752 (1995).
[22] Y. I. Mazur, B. L. Liang, Z. M. Wang, G. G. Tarasov, D. Guzun, and G. J. Salamo, J. Appl. Phys. **101**, 014301 (2007).
[23] R. Heitz, M. Veit, N. N. Ledentsov, A. Hoffmann, D. Bimberg, V. M. Ustinov, P. S. Kop'ev, and Zh. I. Alferov, Phys. Rev. B **56**, 10435 (1997).
[24] O. Brandt, H. Lage, and K. Ploog, Phys. Rev. B **45**, 4217 (1992).
[25] R. P. Leavitt and J. W. Little, Phys. Rev. B **42**, 11774 (1990).
[26] I. Vurgaftman, J. R. Meyer, and L. R. Ram-Mohan, J. Appl. Phys. **89**, 5815 (2001).
[27] B. Vinter, Phys. Rev. B **66**, 045324 (2002).
[28] J. Y. Marzin, M. N. Charasse, and B. Sermage, Phys. Rev. B **31**, 8298 (1985).
[29] A. Krost, J. Bläsing, F. Heinrichsdorff, and D. Bimberg, Appl. Phys. Lett. **75**, 2957 (1999).
[30] D. Leonard, K. Pond, and P. M. Petroff, Phys. Rev. B **50**, 11687 (1994).
[31] J. P. Silveira, J. M. Garcia, and F. Briones, Appl. Surf. Sci. **188**, 75 (2002).
[32] D. B. Migas, P. Raiteri, L. Miglio, A. Rastelli, and H. von Känel, Phys. Rev. B **69**, 235318 (2004).
[33] R. Beanland, Ultramicroscopy **102**, 115 (2005).
[34] M. Hugues, B. Damilano, J.-M. Chauveau, J.-Y. Duboz, and J. Massies, Phys. Rev. B **75**, 045313 (2007).
[35] J. Massies, F. Turco, A. Saletes, and J. P. Contour, J. Cryst. Growth **80**, 307 (1987).
[36] K. Muraki, S. Fukatsu, Y. Shiraki, and R. Ito, Appl. Phys. Lett. **61**, 557 (1992).
[37] M. Mesrine, J. Massies, C. Deparis, N. Grandjean, E. Vanelle, and M. Leroux, J. Cryst. Growth **175-176**, 1242 (1997).
[38] N. Grandjean, J. Massies, and O. Tottereau, Phys. Rev. B **55**, R10189 (1997).
[39] M. Schowalter, A. Rosenauer, and D. Gerthsen, Appl. Phys. Lett. **88**, 111906 (2006).
[40] T. V. Torchynska, J. L. Casas Espinola, L. V. Borkovska, S. Ostapenko, M. Dybiec, O. Polupan, N. O. Korsunska, A. Stintz, P. G. Eliseev, and K. J. Malloy, J. Appl. Phys. **101**, 024323 (2007).